Depth Profile and Material Characteristic

Quantitative Depth Profile Analysis of Micrometer-Thick Multilayered Thin Coatings Using Step-Scan FT-IR Photoacoustic Spectroscopy

Vasilis G. Gregoriou and Sheila E. Rodman

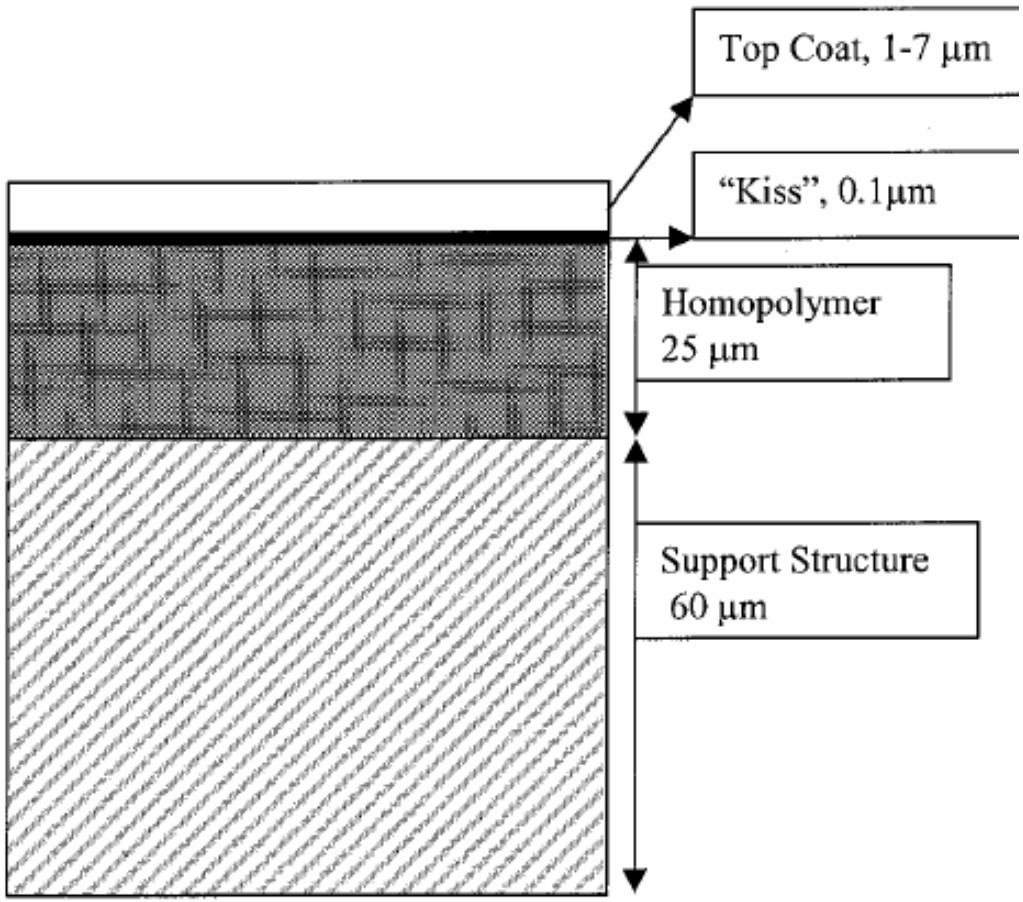

Figure 1. Schematic diagram of the sample under study.

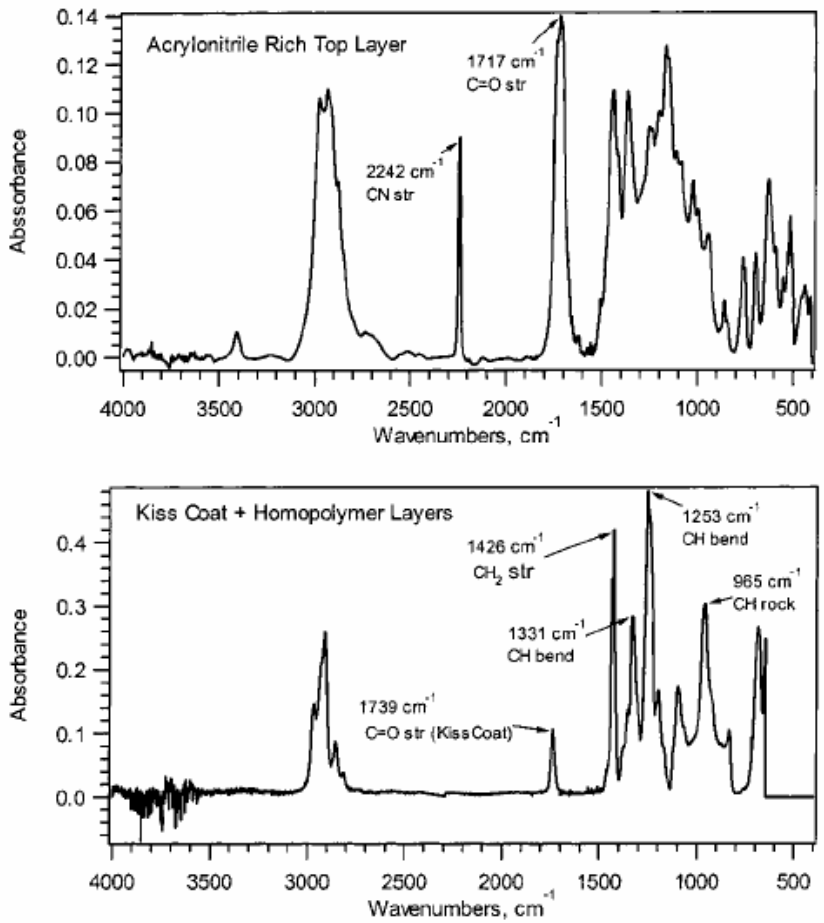

Figure 3. FT-IR reference spectra of the acrylonitrile-rich top coating fluid (upper) and the ultrathin "kiss" coated homopolymer on support (lower).

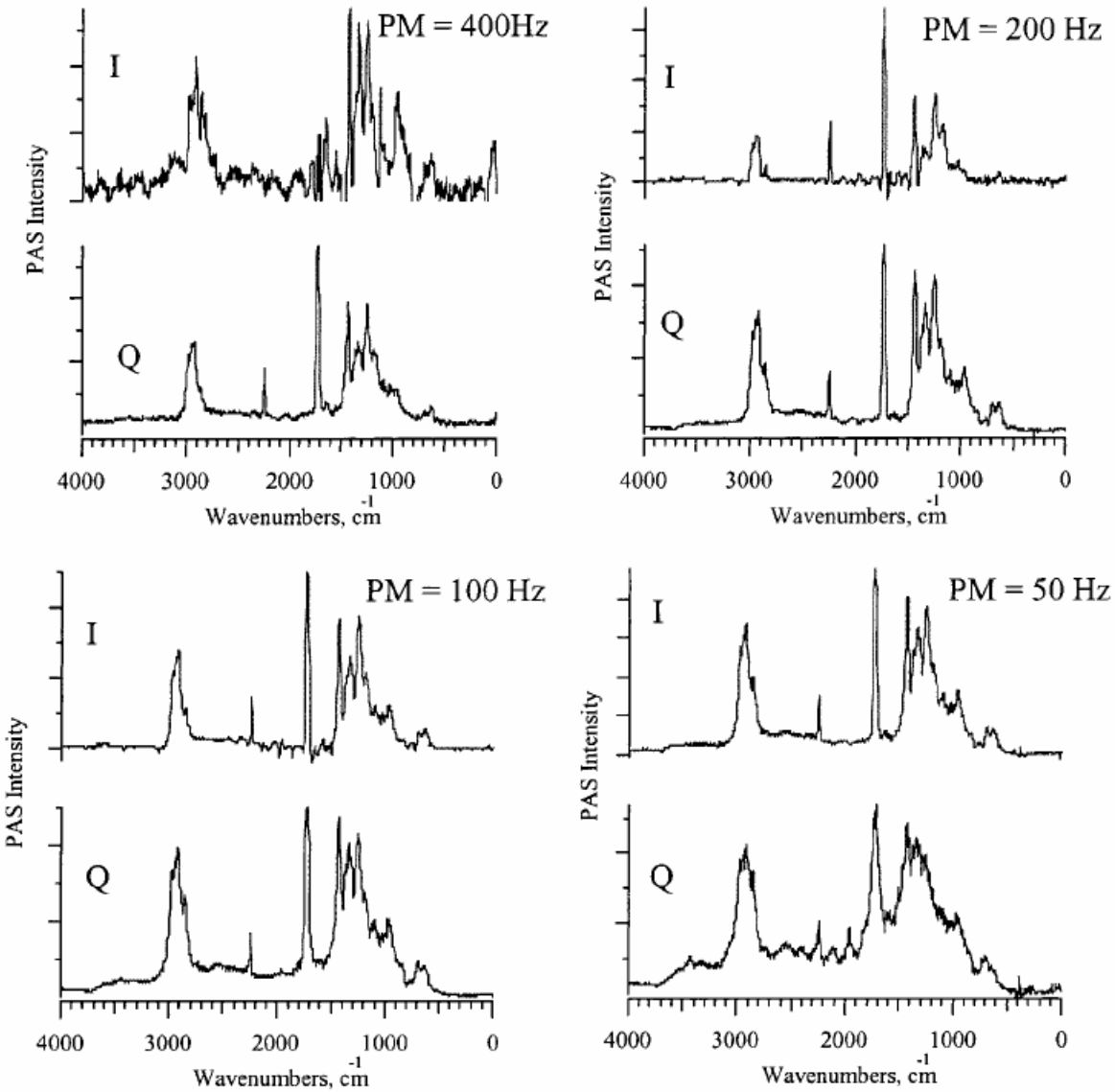

Figure 4. In-phase and quadrature S²FT-IR PAS spectra for various modulation frequencies from 400 (upper left) to 50 Hz (lower right) for a sample with the thickest top layer.

V. G. Gregoriou, S. E. Rodman‡Anal. Chem., 74, **2002,** 2361-2369

Osteoarthritis and Cartilage (2007)

The depth-dependent anisotropy of articular cartilage by Fourier-transform infrared imaging (FTIRI)

Y. Xia Ph.D.*, N. Ramakrishnan Ph.D. and A. Bidthanapally Ph.D.
Department of Physics and Center for Biomedical Research, Oakland University, Rochester, MI 48309, USA

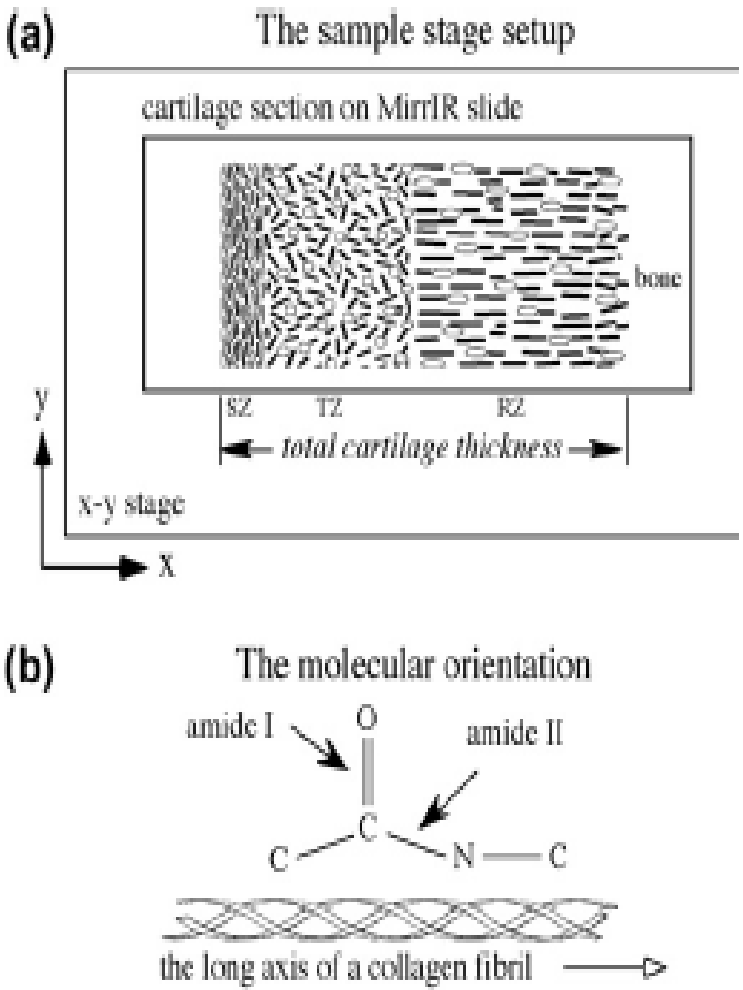

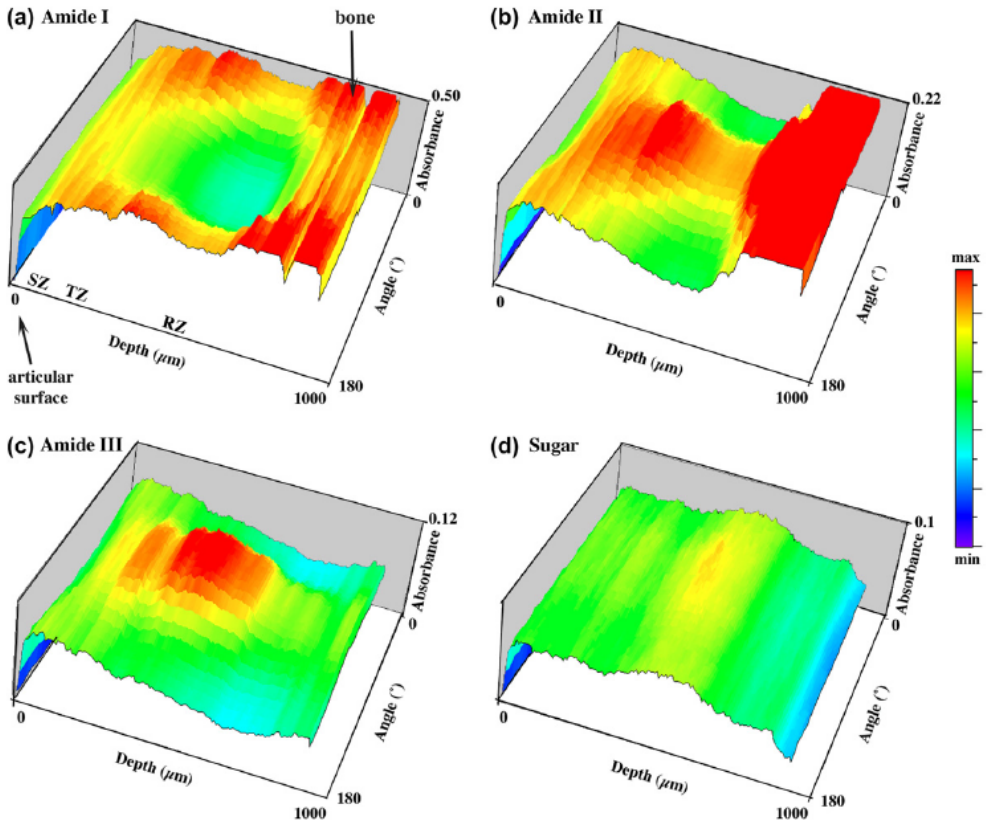

Fig. 5. FTIRI absorbance anisotropy maps: (a) amide I, (b) amide II, (c) amide III and (d) sugar. These maps enable the visualization and summary of the distributions of IR anisotropy at every tissue depth over the angle space of 0–180°. At any particular angle, the profile shows the IR absorption over the entire tissue depth (the profiles in Fig. 4); while at a particular depth, the profile shows the anisotropy of the IR absorption over the 0–180° angle space (the profiles in Fig. 6). (0 μm is the articular surface and 1000 μm is the bone region).

Fig. 1. (a) The orientation of the specimen in the FTIRI instrument (not to scale). The cartilage section was mounted on a MirrIR slide, which was secured on the *x*–*y* moving stage. SZ, TZ, and RZ refer to three histological zones of articular cartilage. (b) The relative orientation of amide I and amide II bonds and the long axes of polypeptide chains in collagen fibril.

Surface enhancement

- SERS is a surface enhanced Raman technique, now roughly 25 years old, and just coming to a state or reliability and huge enhancements – even single molecule
- SEIR(AS) is the IR complement, known for some time as >10X enhancement, but it is also coming on as a more understood and bigger effect due to plasmon resonance

Protein-lipid bilayer assembly on Au-coated surface
Reflection at the surface samples the bound membrane

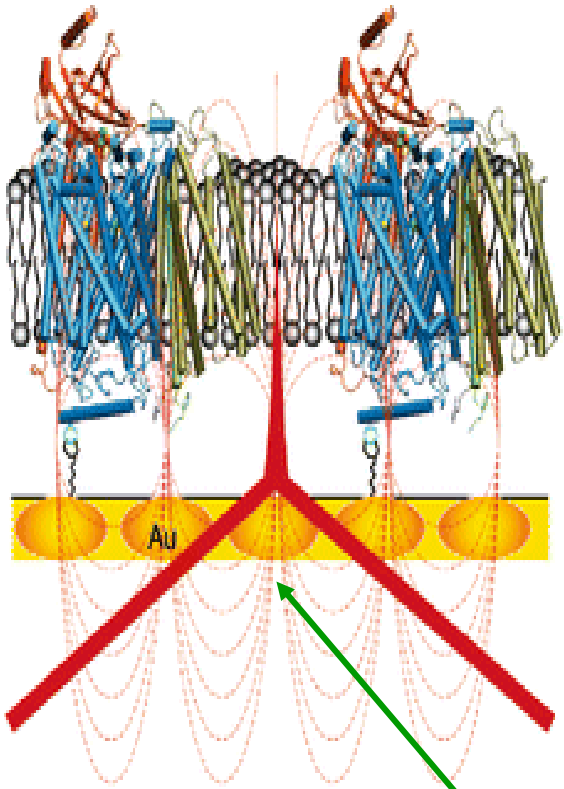

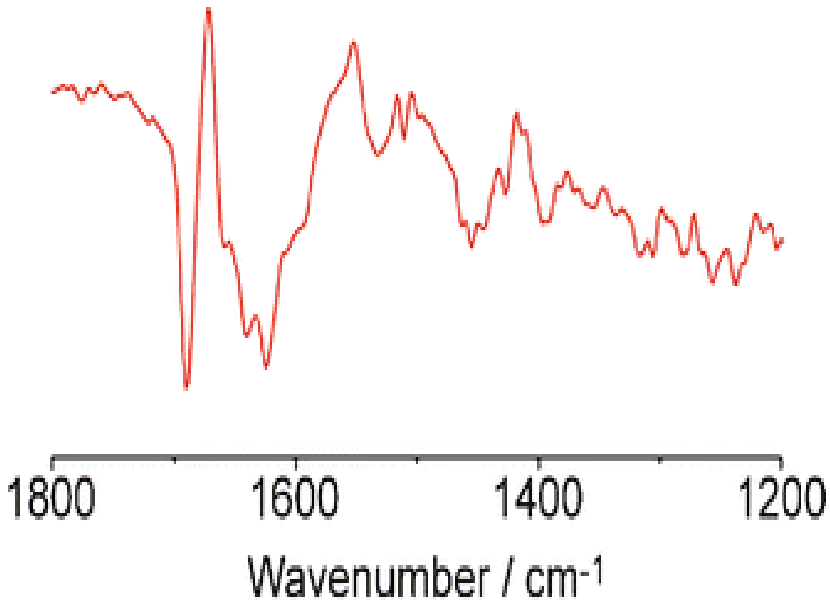

SEIRAS from enhanced field at surface

SEIRS enhancement

Model for electromagnetic enhanceme

Anthraquinone (AQ) on KRS-5

a) 375 ng/cm^2 AQ
b) same with 14 mm Ag colloid
c) 125 ng/cm^2 AQ/14mm Ag
d) 50 ng/cm^2 AQ/14mm Ag

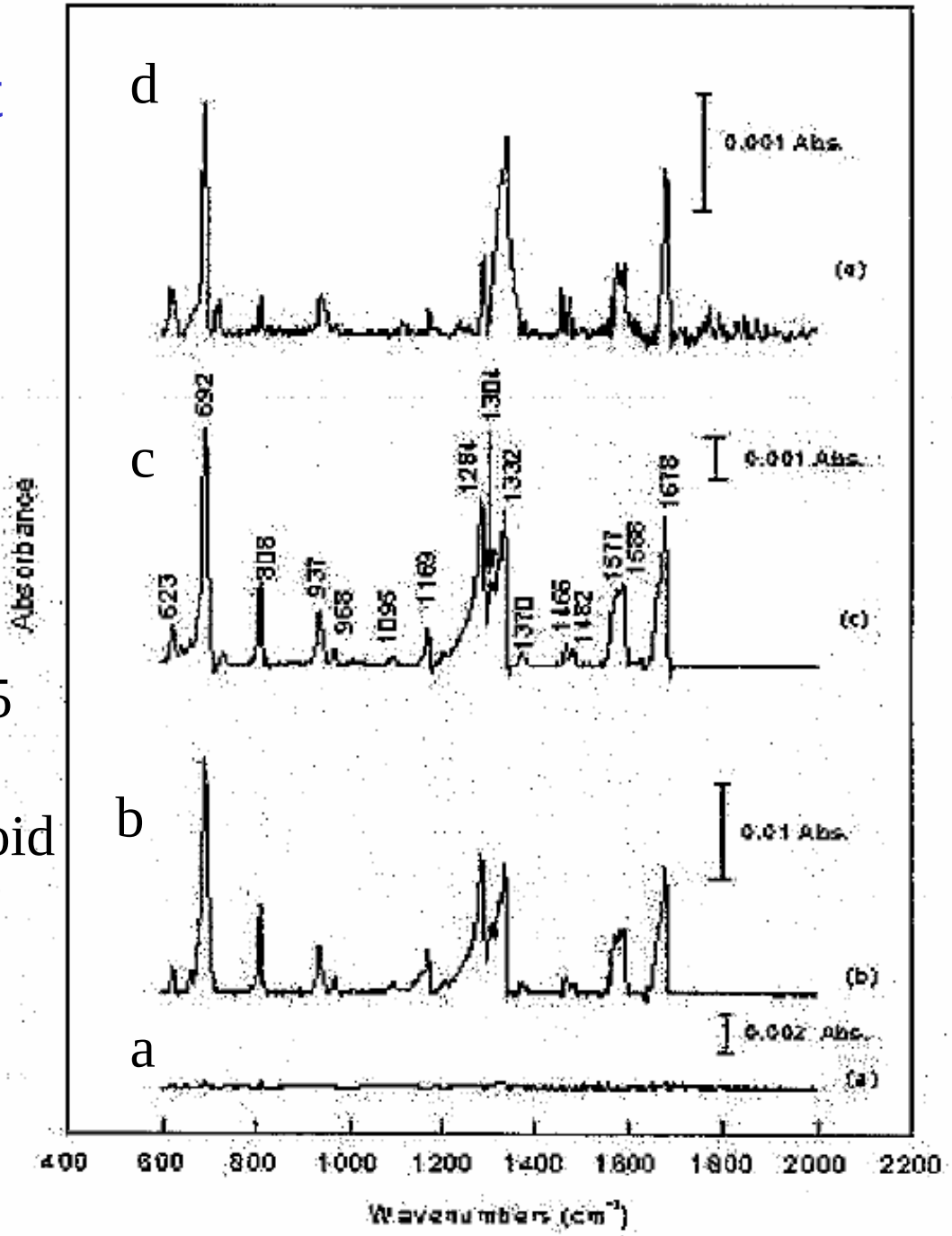

Surface enhanced Infrared absorption:

Protein Functionality probed by SEIR:

The difference spectra reveal changes of the secondary structure induced by rearrangement of the hydrogen-bonded network among the internal amino acid side-chains surrounding the heme chromophore.

Anal Bioanal Chem (2007) 388 47-54

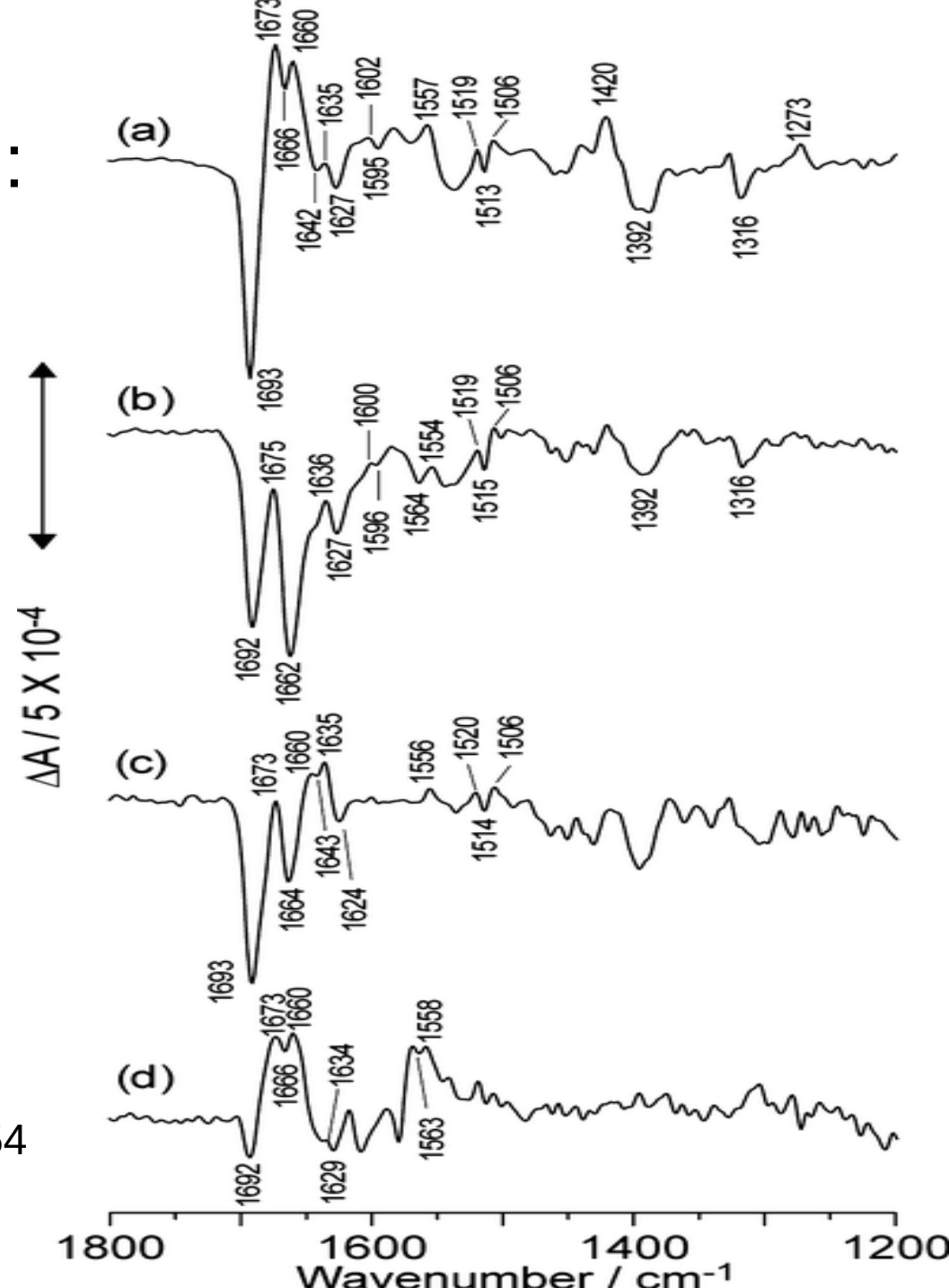

SEIR enhancement depend - Ag nanoparticle geometry:

SEIR enhancement claimed to be 2000 times aided by nanoparticle design to aid interaction

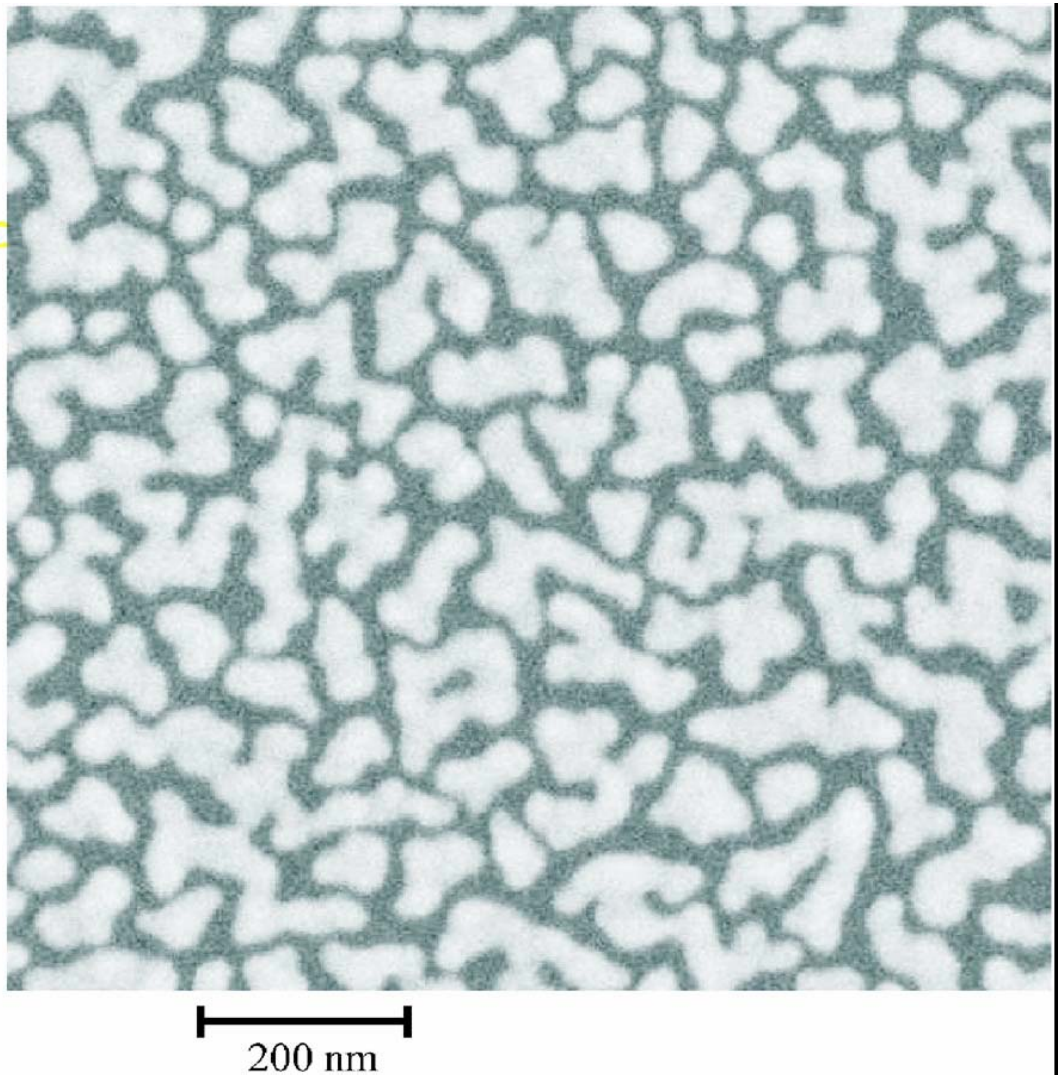

Applied Physics Letters 88, 184104 (2006)

- **Looked at surface,**

  how about a part of the surface?

- **Imaging and microscopy are**

  growth areas

Microscopy/imaging

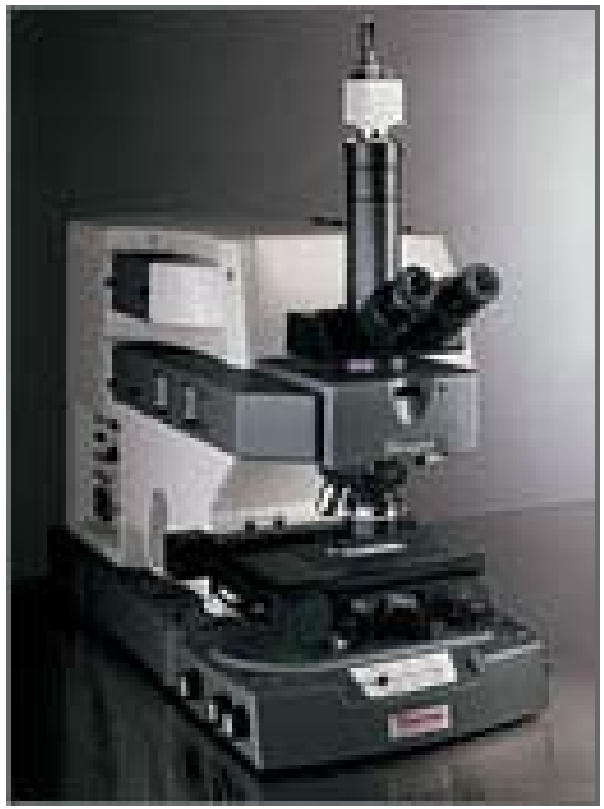

Single point data, aperture limit
Image is spot-to-spot sequential

Imaging system uses focal plane array detectors

Point is to chemically distinguish analyte with spatial resolution
Concept old, now wide spread. Problem - **resolution** limit, favor Raman
Array detectors permit very fast images with spatial rsolved spectra

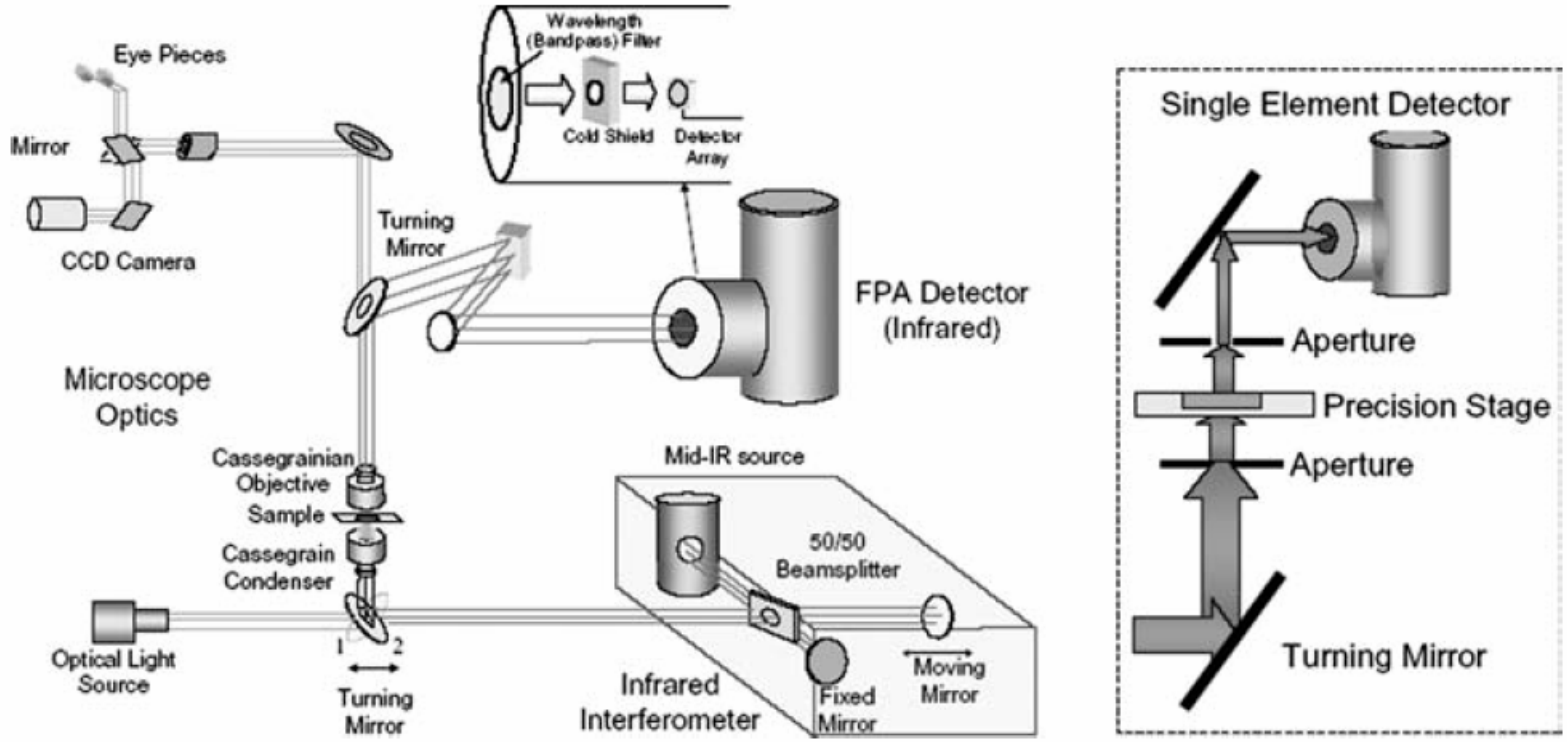

Figure 1 The configuration of a Fourier transform infrared (FTIR) spectroscopic imaging device consists of an interferometer coupled to a microscope and IR-sensitive focal plane array detector. When a conventional, single-element detector is employed (*right*), the microscope is necessarily equipped with apertures and a precision stage. For multichannel detection (*left*), no apertures are required.

FOURIER TRANSFORM INFRARED VIBRATIONAL SPECTROSCOPIC IMAGING: Integrating Microscopy and Molecular Recognition*IraW. Levin and Rohit Bhargava
Annu. Rev. Phys. Chem. 2005. 56:429–74

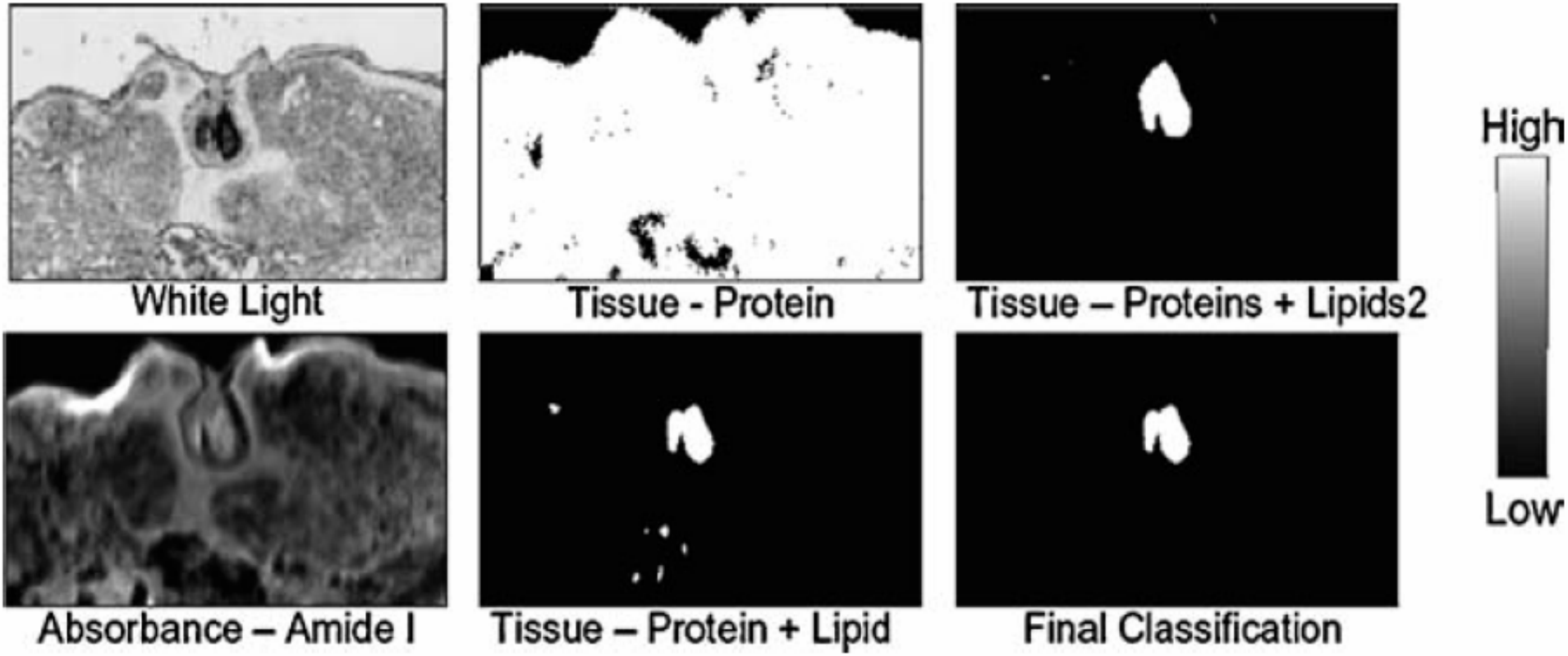

Figure 5 An unstained sample of human skin tissue is spectroscopically imaged and segmented using an automated numerical analysis procedure. The brightfield microscopy image (*top*, *left*) of the sample demonstrates several different structures. The Amide I absorbance intensity (*bottom*, *left*) can be employed to differentiate tissue from empty space (*top*, *middle*). The further inclusion of specific absorbance modes helps to segment finally (*bottom*, *right*) the sebaceous gland components within the

IraW. Levin and Rohit Bhargava Annu. Rev. Phys. Chem. 2005

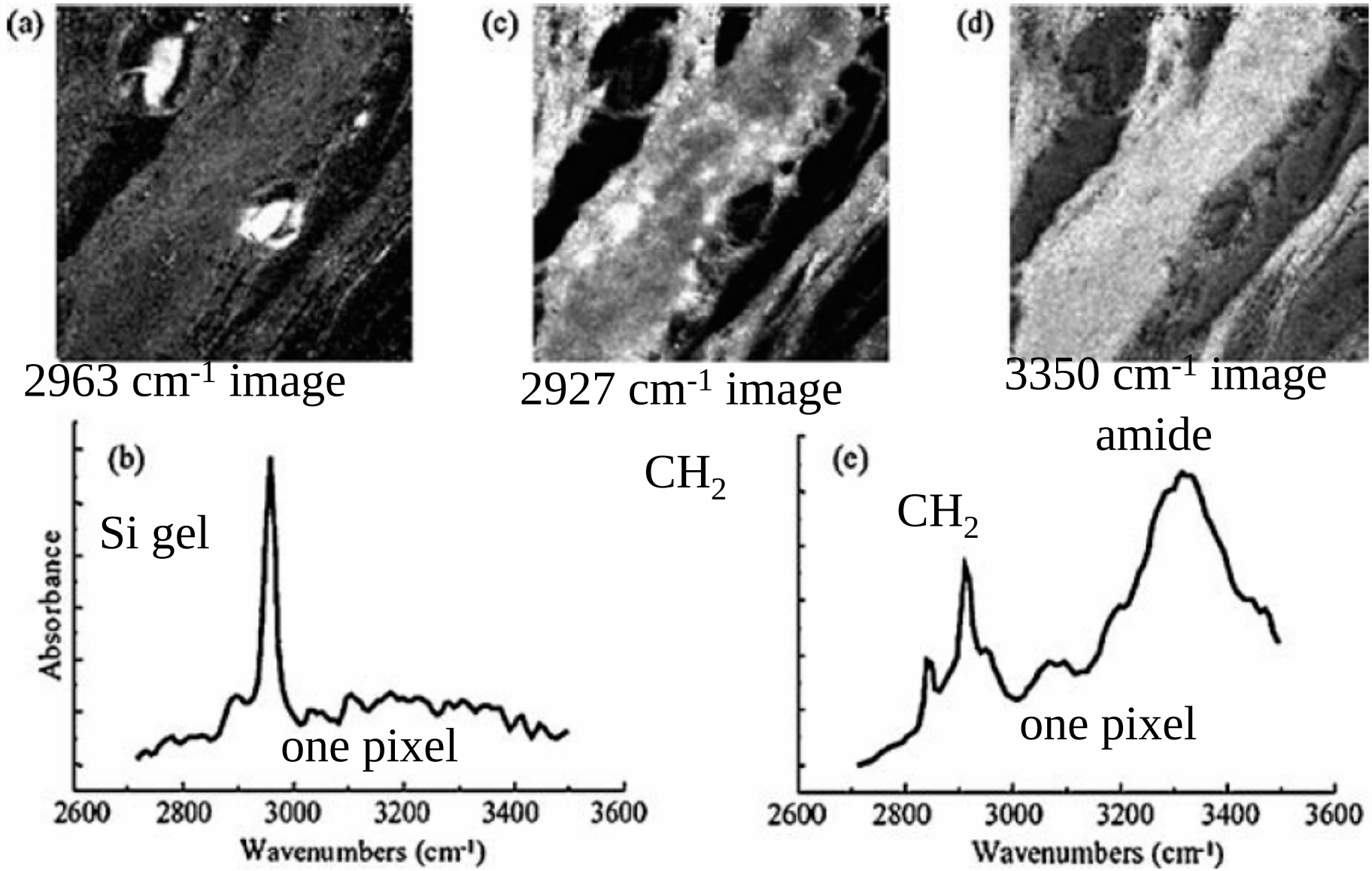

Figure 8 Infrared (IR) spectroscopic images and spectra of human breast implant capsular tissue. Vacuoles in the sample appear consistently as nonabsorbing black

IraW. Levin and Rohit Bhargava Annu. Rev. Phys. Chem. 2005

Bone imaging

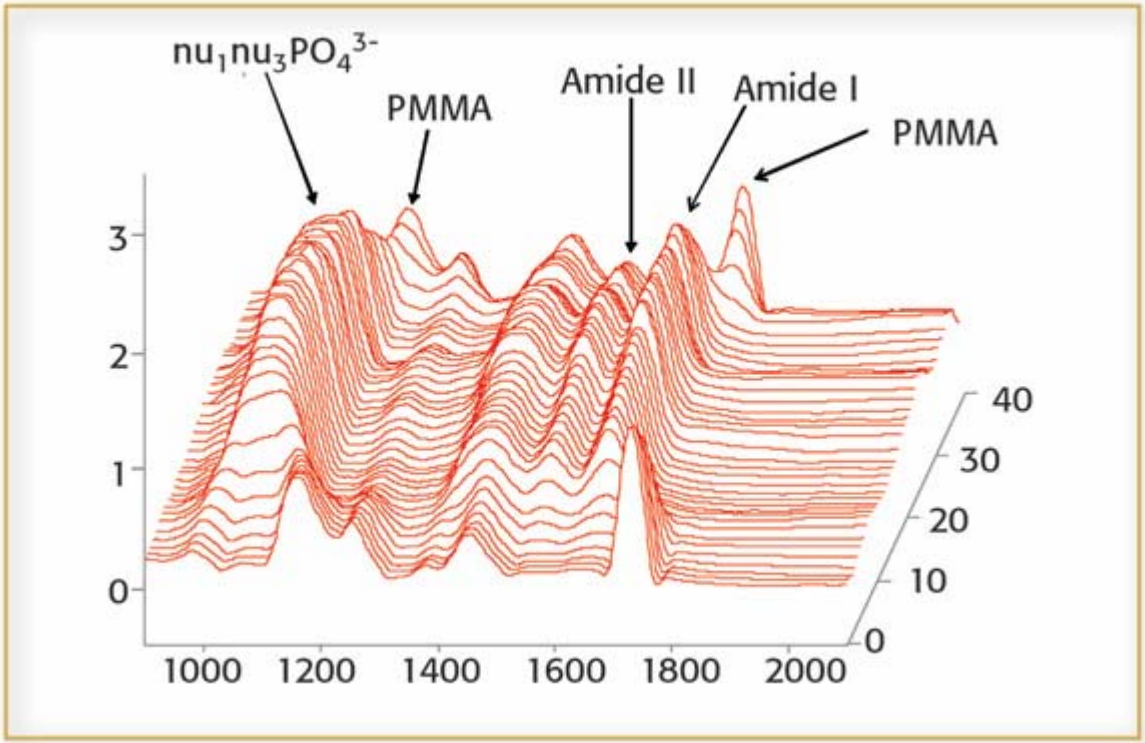

IR fingerprints change at each location in the tissue. Key: PMMA: polymethyl-methacrylate; amide I and amide II bands.

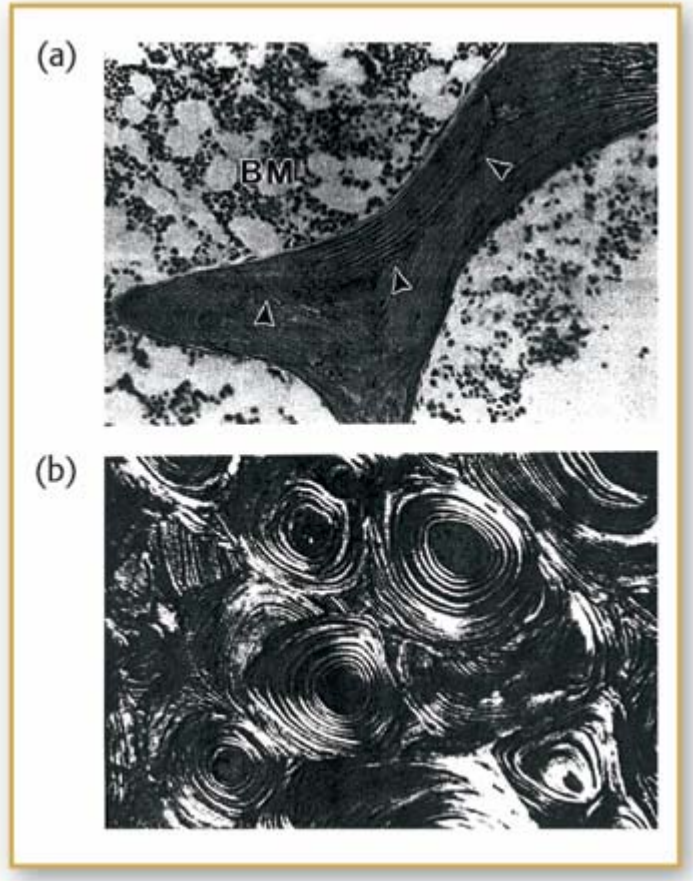

Images of (a) trabecular and (b) cortical bone.

Paschalis, . . . Mendelsohn, *J. Bone Mineral Res.* **19**, 2000–(2004)

A. L. Boskey, . . . R. Mendelsohn, *Osteoporosis Int.* (in press).

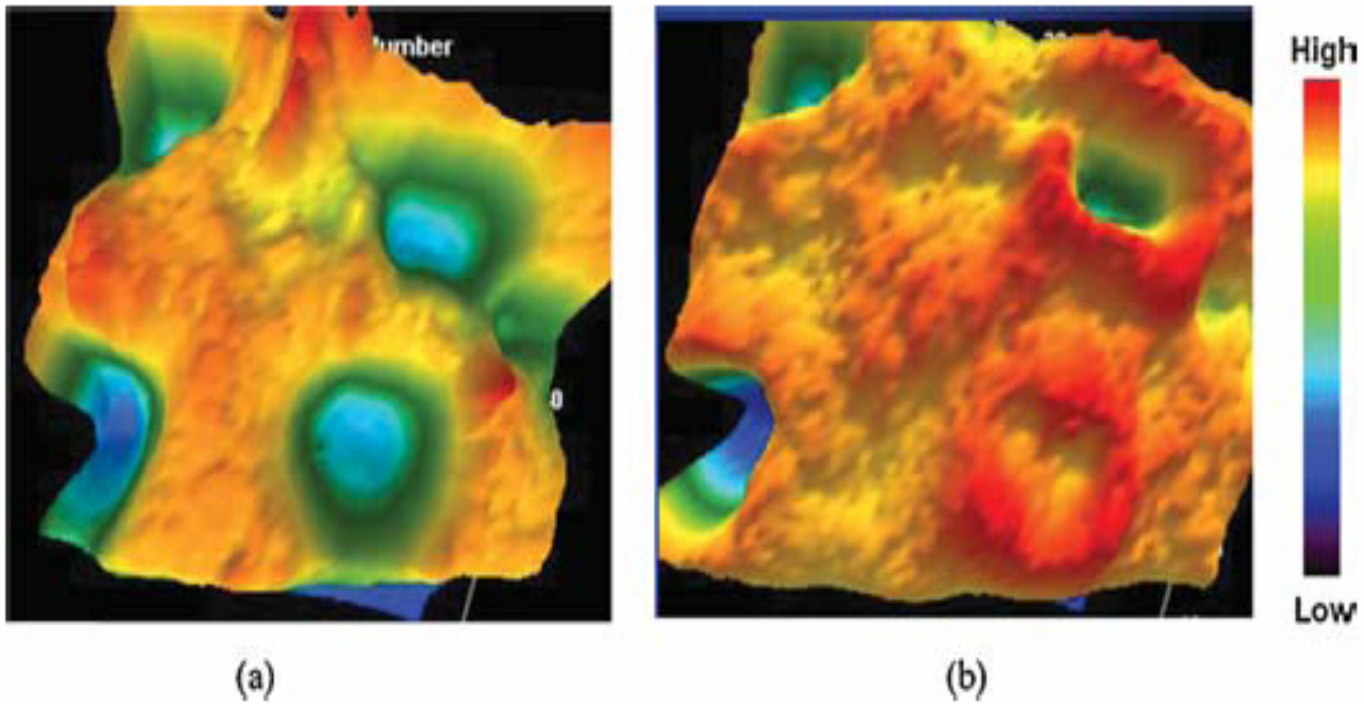

Figure 7 (*a*) Infrared (IR) color scale images of a normal bone human iliac crest biopsy. The spatial distribution hydroxyapatite generated from the integrated intensities of the phosphate $\nu 1$, $\nu 3$ contour across the 64×64 array of the HgCdTe (MCT) elements is an indication of the mineral present in the sample. The elliptical structure corresponds to a single osteon. The color coding used to generate the images is indicated on the scale to the right of the Figure. (*b*) IR color scale image of the spatial distribution of protein generated from the integrated intensities of the Amide I mode

Richard Mendelsohn, Rutgers

Amyloid deposit identification with FTIR

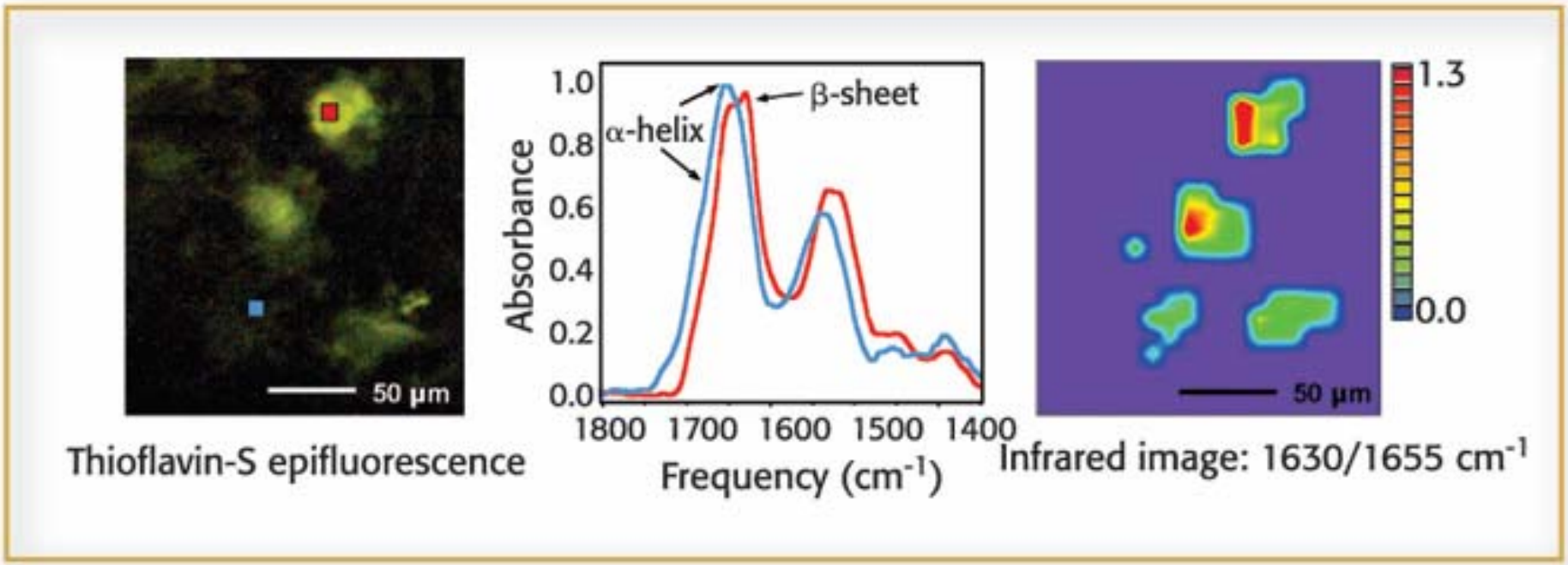

Amyloid deposits in neuronal cells. Evidence of amyloid formation in neuronal cells infected with spirochetes

J. Miklossy, et al., *Neurobiol. Aging*

From: Infrared Tissue Imaging Applications Growing in Biomedical Research and Diagnosis –Sharon Williams, Spectroscopy 2006

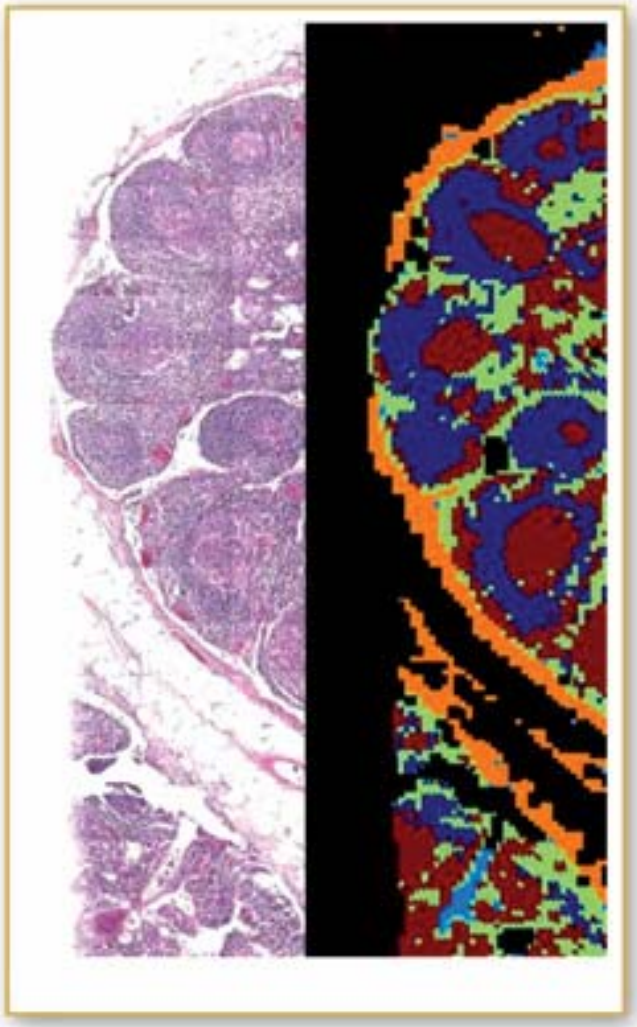

Stained section (left) and spectral pseudo color map (right) of lymph node.

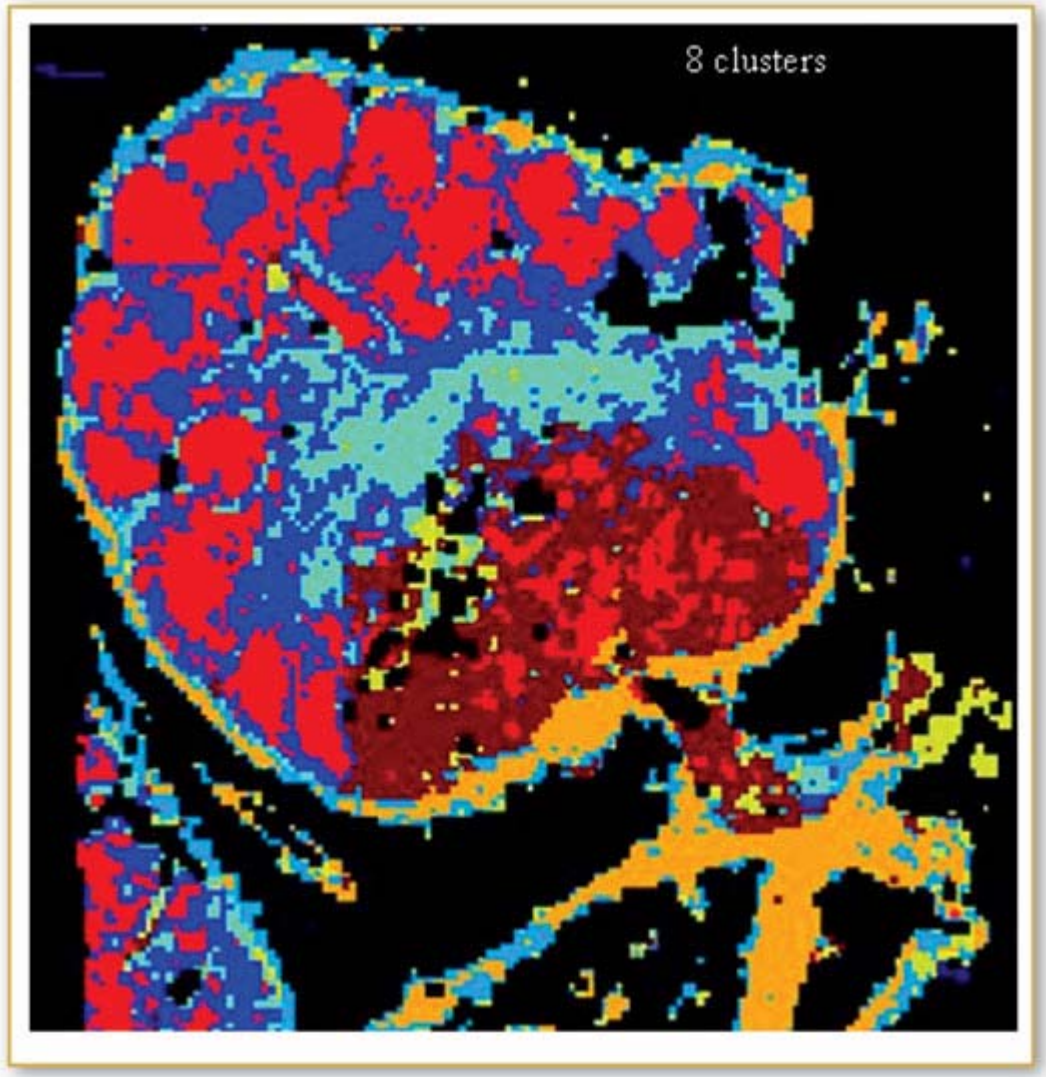

Lymph node with colon cancer metastatis.

M. Diem, M. Romeo, et al., *Analyst*. **129(10)**, 880–885. (1994–2004).
M.J. Romeo and M. Diem, *Vibrational Spectrosc*. **38**, 115–119. (2005).